Irreversible phase transitions  in a dimer - monomer - monomer reaction model

# Irreversible phase transitions in a dimer–monomer–monomer reaction model

Ezequiel V Albano†

Instituto de Investigaciones Fisicoquímicas Teóricas y Aplicadas (INIFTA), Facultad de Ciencias Exactas, Universidad Nacional de La Plata, Sucursal 4, Casilla de Correo 16, (1900) La Plata, Argentina

**Abstract.** A multiple-reaction irreversible surface reaction model involving one dimer ($B_2$) and two different monomers (A and C) is proposed and studied by means of Monte Carlo simulations. This dimer–monomer–monomer (DMM) model is suitable to investigate, on the one hand, the influence caused by dimer traces on the behaviour of the monomer–monomer (MM) model, i.e. $A + C \rightarrow AC$, and on the other hand, the effects of monomer traces on the dimer–monomer (DM) model, i.e. $\frac{1}{2}B_2 + A \rightarrow AB$, which mimics the catalytic oxidation of carbon monoxide (B is O, A is CO and AB is CO). The DMM model exhibits irreversible phase transitions (IPTs) between poisoned states with the surface saturated by adsorbed species and reactive regimes with production of AB, AC and BC. The critical points at which second- and first-order IPTs take place are determined. Second-order IPTs belong to the universality class of directed percolation. However, universality is not found to hold at first-order IPTs due to short-range correlations. So, each critical point has its own set of critical exponents. These exponents smoothly cross over from values characteristic of the DM model to those of the MM model.

## 1. Introduction

Stochastic lattice-gas models have very recently received growing attention in connection with the study of far-from-equilibrium reaction processes [1–3]. These processes include heterogeneously catalysed reactions which often exhibit irreversible phase transitions (IPTs) between reactive steady states and poisoned states. By analogy to thermodynamic phase transitions, this term means physically that the behaviour of the system changes qualitatively when some control parameter, such as the temperature or the pressure, is finely tuned close to a critical point. If the change of the order parameter is stepwise at the critical point, the IPT is of first order. If the change is continuous the IPT is of second order.

Within this context the dimer–monomer (DM) model as proposed by Ziff *et al* [4] has been studied extensively using a great variety of theoretical approaches, see e.g. [5–22] and references therein. The DM model for the reaction $A + \frac{1}{2}B_2 \rightarrow AB$ exhibits two IPTs: one of second order at low partial pressure of the monomer and the other of first order at higher pressures. For intermediate pressures, between the critical points, a stationary reactive state is observed [4]. Also, the monomer–monomer (MM) model, $A + C \rightarrow AC$, has been studied recently [2, 3, 5, 23]. For this model the surface is always poisoned with either monomer A or C, except when the partial pressure of both species is the same and a reactive state is observed. The IPTs from the poisoned states to the reactive regime are of first order.

† E-mail address: ealbano@isis.unlp.edu.ar

The aim of this work is to propose and study, by means of the Monte Carlo method, a multiple-reaction surface reaction model, namely a dimer–monomer–monomer (DMM) model. The DMM model is based upon both the DM and the MM models. Interest in the study of multiple reaction systems is due to many reasons [24]. In fact, heterogeneously catalysed reactions deal with mechanisms consisting of a vast number of elementary processes. Since the handling of such a large number of mechanisms imposes severe problems, the usual procedure is to rationalize their study. Within this context, the study of the DMM model allows us to investigate the influence of C-traces (B-traces) in the irreversible behaviour of the DM model (MM model), respectively. That is, the influence of contaminants on the critical behaviour of the well known IPTs characteristic of both the DM and MM processes can be studied. Furthermore, the DMM model itself exhibits an interesting and rich irreversible critical behaviour.

The paper is organized as follows. The DMM model is described and discussed in section 2. Section 3 is devoted to the description of the Monte Carlo simulation method. Results are presented and discussed in section 4. Finally, in section 5 we state our conclusions.

## 2. The dimer–monomer–monomer surface reaction model

The reaction scheme studied in this work is based upon the well known Langmuir–Hinshelwood mechanism for which the reactants must be adsorbed on the catalytic surface, so

$$A(g) + (*) \rightarrow A(a) \tag{1a}$$

$$B_2(g) + 2(*) \rightarrow 2B(a) \tag{1b}$$

$$C(g) + (*) \rightarrow C(a) \tag{1c}$$

$$A(a) + B(a) \rightarrow AB(g) + 2(*) \tag{1d}$$

$$A(a) + C(a) \rightarrow AC(g) + 2(*) \tag{1e}$$

$$C(a) + B(a) \rightarrow CB(g) + 2(*) \tag{1f}$$

where $(*)$ denotes a vacant site on the catalyst surface, while (a) and (g) indicate adsorbed and gas phase species, respectively. Surface sites can be empty or occupied by A, B or C species with average coverages $\theta_A$, $\theta_B$ and $\theta_C$, respectively. The gas phase in contact with the catalyst surface is assumed to be kept at constant pressure and composition of A, $B_2$ and C molecules. So, the respective rate of arrival and subsequent sticking coefficients are $Y_A$, $Y_B$ and $Y_C$, which are normalized so that $Y_A + Y_B + Y_C = 1$, and consequently the model has only two parameters, namely $Y_A$ and $Y_C$. For $Y_C = 0$, equations (1a), (1b) and (1d) correspond to the DM model: $A + \frac{1}{2}B_2 \rightarrow AB$; for $Y_A = 0$, equations (1b), (1c) and (1f) correspond to the DM model: $C + \frac{1}{2}B_2 \rightarrow CB$, and for $Y_B = 0$, equations (1a), (1c) and (1e) correspond to the MM model: $A + C \rightarrow AC$.

## 3. Description of the Monte Carlo simulation method

The DMM reaction model was simulated on the homogeneous square lattice of side $L = 252$ lattice units using periodic boundary conditions. The simulation algorithm may be briefly summarized as follows: a site, say site 1, of the catalytic surface is initially selected at random. If site 1 is occupied the trial ends but if site 1 is empty an A, $B_2$ or C species is selected at random with probabilities $Y_A$, $Y_B$ and $Y_C$, respectively. If the selected species is

a dimer ($B_2$) a nearest-neighbour (NN) site, say site 2, is also selected at random. If site 2 is occupied the trial ends because there is no place for dimer adsorption. Otherwise, if site 2 is also empty the dimer is adsorbed. Otherwise, if the selected species is a monomer, it is adsorbed on site 1. When a species becomes adsorbed its nearest-neighbour (NN) sites must be examined in order to account for the reactions described by $(1d)$–$(1f)$. These reactions are assumed to take place only when the involved species are adsorbed on NN sites. If, after adsorption, more than one type of reaction is possible, the reaction path is selected at random.

The Monte Carlo time unit ($t$) involves $L^2$ trials, so each site of the lattice will be visited once, on average, during each time unit. Additional simulation details can be found in earlier publications of both the DM [4] and the MM [5] models, respectively.

Simulations are performed on a PowerXplorer, supplied by Parsytec (Germany), built with eight PowerPC 601 application processors (32 MB RAM each) and eight T805 VCP communication processors. The computer system allows the development of fully parallelized codes. Evaluation of a single epidemy ($10^6$ averages, see section 3.2) close to criticality typically requires one CPU day.

## 4. Results and discussion

### 4.1. The phase diagram of the DMM model

For $Y_C = 0$, the DMM model is mapped onto the DM model [4], so equations $(1a)$, $(1b)$ and $(1d)$ correspond to the DM model $A + \frac{1}{2}B_2 \rightarrow AB$. That is, (see figure 1), for $Y_{1A} \leqslant 0.3905$ ($Y_{2A} \geqslant 0.525$) the surface becomes fully covered by B (A) species, respectively. So, within these regimes the system becomes irreversibly poisoned by the reactants and the production of AB stops. These poisoned states are unique in the sense that they correspond to a single configuration of the covered surface. Within the interval $Y_{1A} \leqslant Y_A \leqslant Y_{2A}$ one observes sustained production of AB and therefore both $Y_{1A}$ and $Y_{2A}$ are critical points at which IPTs between the reactive regime and poisoned states of the surface take place. The transition at $Y_{1A}$ is continuous (second order) while the transition at $Y_A$ is discontinuous (first order). Also, for $Y_A = 0$, equations $(1b)$, $(1c)$ and $(1f)$ correspond
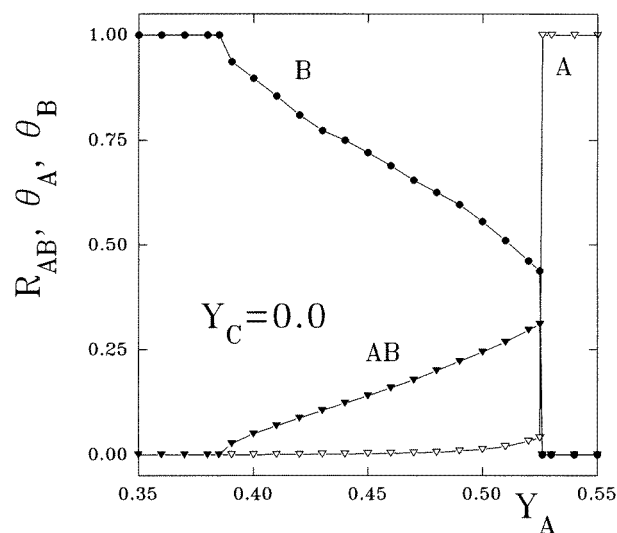


**Figure 1.** Plots of the reactant coverages $\theta_A$, $\theta_B$ and the rate of AB production ($R_{AB}$) versus $Y_A$ obtained keeping $Y_C = 0$, i.e. the DM model. Note the existence of second- and first-order IPTs at $Y_{1A} = 0.3905$ and $Y_{2A} = 0.525$, respectively.
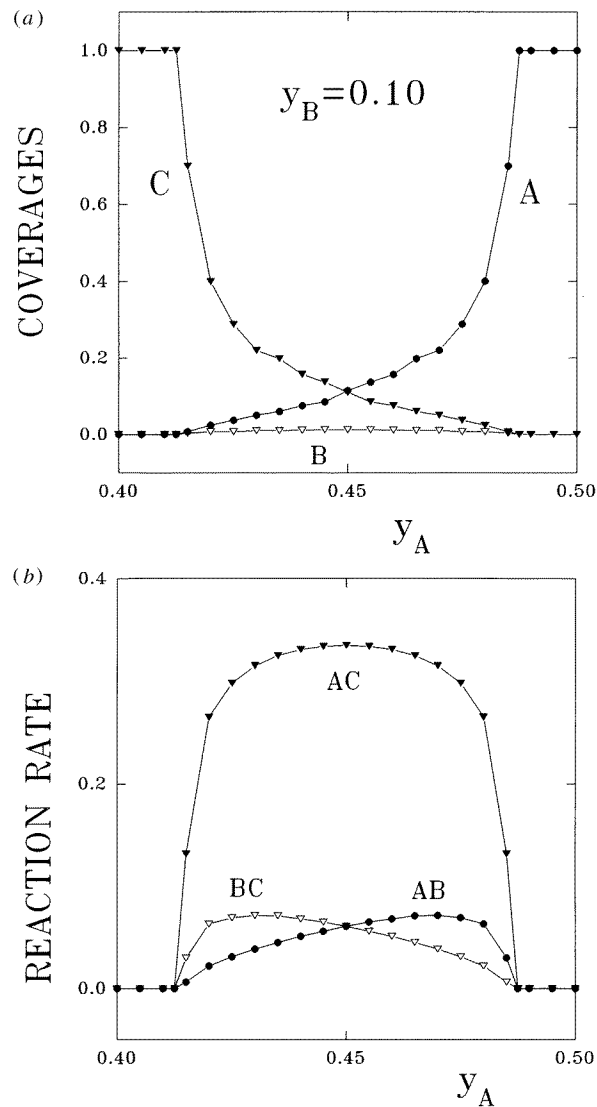
(*a*)



(*b*)
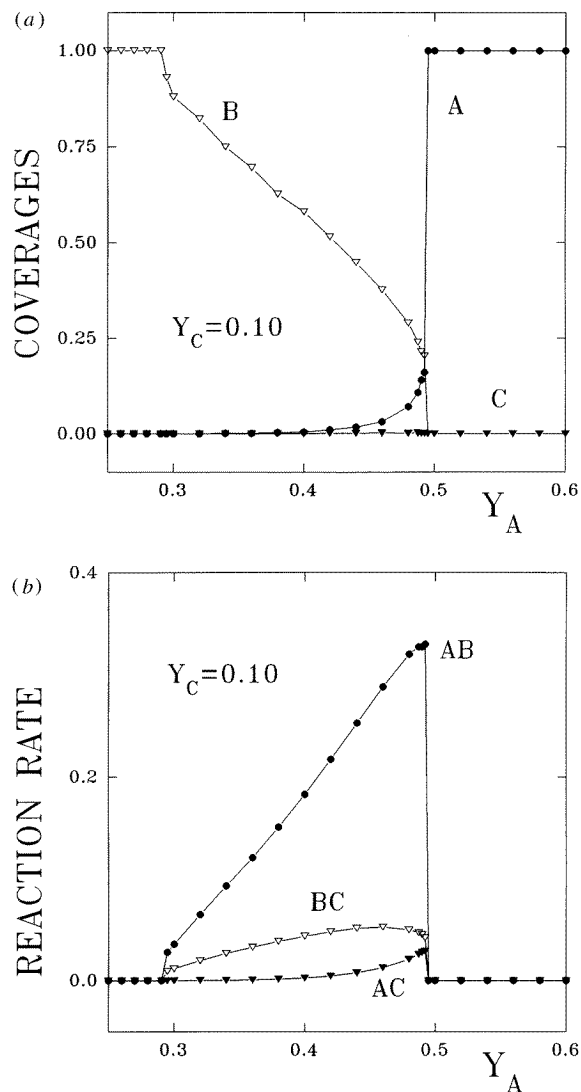


**Figure 2.** (*a*) Plots of the reactant coverages $\theta_A$, $\theta_B$ and $\theta_C$ and (*b*) the reaction rates $R_{AB}$, $R_{BC}$ and $R_{AC}$ versus $Y_A$ obtained keeping $Y_C = 0.10$. Note the existence of second- and first-order IPTs at $Y_{1A} = 0.2905$ and $Y_{2A} = 0.495$, respectively.

to the DM model $C + \frac{1}{2}B_2 \rightarrow CB$ and the corresponding phase diagram is the same as that shown in figure 1 but now A has to be replaced by C. For additional details on the DM model see [4–22].

For $Y_B = 0$, equations (1*a*), (1*c*) and (1*e*) correspond to the MM model $A + C \rightarrow AC$. Now there is a single (trivial) critical point at $Y_{1C} = Y_{1A} = \frac{1}{2}$ such as for $Y_C < Y_{1C}$ ($Y_C > Y_{1C}$) the surface becomes irreversibly poisoned by A (species C), respectively. The IPT at $Y_{1C}$ is of first order. It is expected that, just at criticality, a sustained reaction with AC production can only take place on the infinite lattice [5, 23]. For additional details on the MM model see [2, 3, 5, 23].

Due to the presence of a small fraction of C species in the gas phase the IPTs become slightly shifted (see figure 2 for $Y_C = 0.10$) and the phase diagram is similar to that of

**Figure 3.** (*a*) Plots of the reactant coverages $\theta_A$, $\theta_B$ and $\theta_C$ (*b*) the reaction rates $R_{AB}$, $R_{BC}$ and $R_{AC}$ versus $Y_A$ obtained keeping $Y_B = 0.10$. Note the existence of first-order IPTs at $Y_{1A} = 0.405$ and $Y_{2A} = 0.495$, respectively.

the DM model shown in figure 1. In fact, the second-order IPT occurs at $Y_A^* = Y_{1A} - Y_C$, where $Y_{1A}$ is the critical point of the DM model. So, the transition takes place at a well determined total pressure of monomers given by $Y_A + Y_C = Y_{1A} \cong 0.3905$, suggesting that both monomers play the same role. However, the surface coverage with the monomer with smaller partial pressure (C in this example) is negligible (see figure 2(*a*)) because this species is quickly removed from the surface via two reaction paths given by equations (1*e*) and (1*f*), see also figure 2(*b*). Also, within the reactive regime it is found that $R_{BC} > R_{AC}$ because B are the majority species on the surface. On the other hand, now $R_{AB}$ is slightly enhanced due to the presence of C species as compared with the pure DM model with $Y_C = 0$ (figure 1).

The introduction of a small contamination with dimers causes the zero-width reaction window of the MM model to become opened, as is shown in figure 3 for $Y_B = 0.10$. The
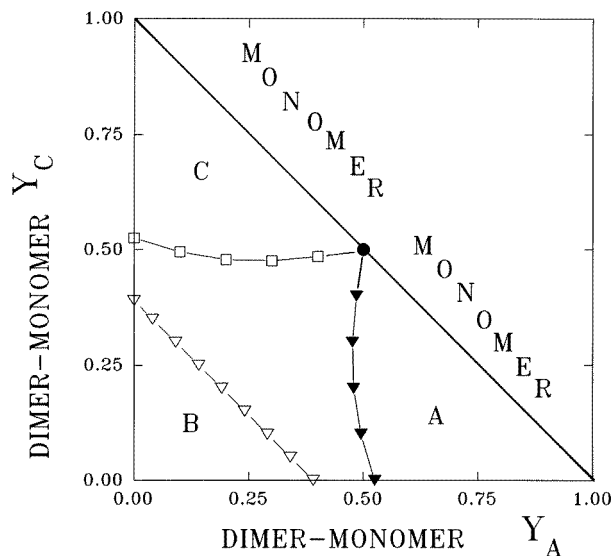
**Figure 4.** Plot of the critical points $Y_C$ versus $Y_A$ of the DMM model. ($\triangledown$) second-order IPTs, ($\blacktriangledown$) and ($\square$) first-order IPTs. ($\bullet$) shows the location of the IPT of the MM model.

phase diagram is now symmetric around the point $Y_A^S = Y_{1A} - \frac{1}{2}Y_B$, where $Y_{1A} = \frac{1}{2}$ is the critical point of the MM model in the absence of dimers. The IPTs at the boundaries of the reaction window are of first order.

As follows from figures 2 and 3, the poisoned states of the DMM model are unique, in the sense that the catalyst surface becomes saturated by a single species, namely A, B or C. This behaviour is in contrast to that observed for the monomer–dimer–dimer model, where non-unique poisoned states are found [25–27].

Scanning both $Y_A$ and $Y_C$ one can construct the complete phase diagram of the DMM model as shown in figure 4. The open triangles indicate second-order IPTs from poisoned states with B species and the reactive regime with sustained production. Open squares and full triangles show first-order IPTs from the reactive regime to poisoned states with C and A species, respectively. Also, the full circle shows the critical point of the MM model.

### 4.2. The time-dependent critical behaviour of the DMM model

The determination of 'static' exponents in irreversible reaction systems, such as the order parameter critical exponent, the correlation length exponent, the susceptibility exponent, etc, is quite difficult and rather inaccurate due to finite-size effects and metastabilities of the system. In fact, for $t \to \infty$ the final state of all finite systems must be a poisoned one. It has been established that a fruitful approach to overcome this shortcoming is to perform an epidemic analysis and to calculate exponents related to the time-dependent critical behaviour of the process [13, 15, 16, 21, 26, 27]. For this purpose one proceeds as follows: simulations start with lattices completely poisoned except for a blob of empty sites placed close to the centre of the sample. Then, the time evolution of the blob embedded in the poisoned state is monitored. The measured quantities are: (i) the survival probability $P(t)$, that is, the probability that the sample was not poisoned after $t$ time steps and (ii) the average number of empty sites $N(t)$. The number of empty sites $N(t)$ is averaged over all samples, including those that have already been poisoned. Averages are taken over $K$ independent realizations (or runs). Each run proceeds until some fixed maximum time $t_M$, unless the sample becomes poisoned before $t_M$. Typically we used $K = 10^6$, $t_M = 10^3$ and blobs of

different size, between two and six empty sites (critical points and critical exponents are found to be independent of the blob size). The sample size is taken large enough in order to prevent empty sites from reaching the boundaries. Using this procedure the obtained results are free of undesired finite-size effects. At the critical point and in the $t \to \infty$ limit it is expected that the following scaling laws should hold [28]:

$$P(t) \propto t^{-\delta} \tag{2}$$

and

$$N(t) \propto t^{\eta}. \tag{3}$$

So, just at criticality, the asymptotic slopes of log–log graphs of equations (2) and (3) define the dynamic critical exponents $\delta$ and $\eta$, respectively, while slightly off-criticality deviations from the asymptotic linear behaviour are expected to occur. The latter property also allows us a precise determination of the critical threshold. Since we are mainly interested in the critical behaviour of the DMM model close to the first-order critical threshold, we do not have to evaluate the average mean square distance of spreading [15, 16].

It has been established that second-order IPTs belong to the universality class of directed percolation (DP), or equivalently to Reggeon field theory [13, 28], e.g. with dynamic critical exponents $\eta \cong 0.214 \pm 0.008$ and $\delta \cong 0.460 \pm 0.006$. Epidemic analysis performed along the second-order critical line shown in figure 4 confirms that these IPTs also belong to the universality class of DP.

Epidemic analysis has also been performed along the first-order critical lines shown in figure 4. These studies are more interesting since one should expect the absence of universality. Figures 5(*a*) and (*b*) show log–log plots of $N(t)$ and $P(t)$ versus $t$ obtained taking $Y_C = 0.10$ and scanning $Y_A$ close to criticality. The straight line behaviour obtained in both figures for $Y_A = 0.4950$ is the signature of criticality, while upward (downward) deviations for $Y_A = 0.4945$ ($Y_A = 0.4955$) indicate supercritical (subcritical) behaviour, respectively. The results of epidemic analysis performed at other critical points are summarized in figures 6(*a*) and (*b*) and the critical exponents obtained are listed in table 1.

The reported critical exponents (see table 1) clearly show that these first-order IPTs do not belong to the DP universality class, as expected. Furthermore, the exponents $\eta$ are negative while for DP they are positive. As has already been discussed, for $Y_C = 0$ the DMM model is mapped onto the DM model. So, the obtained critical exponents are in excellent agreement with previously reported values (see the two first rows of table 1). On the other

**Table 1.** List of critical points and critical exponents $\delta$ and $\eta$, for the first-order IPTs of the DMM model, defined according to equations (2) and (3). PW $\equiv$ present work. The quoted error bars merely reflect the statistical error.

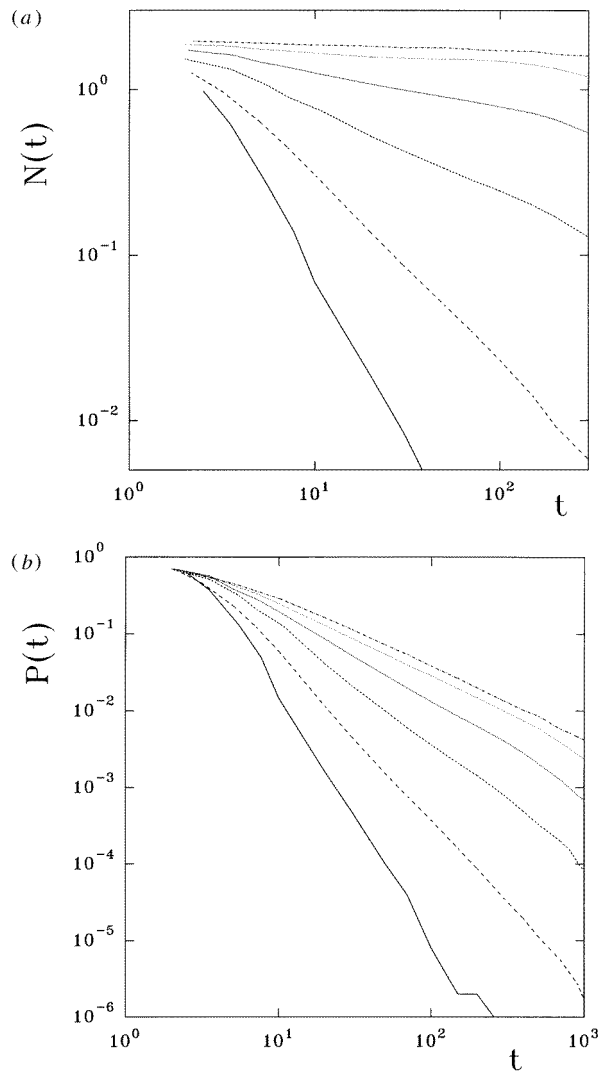| $Y_A$ | $Y_C$ | $\delta$ | $\eta$ | Reference |
|---|---|---|---|---|
| 0.525 | 0.0 | $3.7 \pm 0.2$ | $-2.4 \pm 0.2$ | [15] |
| 0.525 | 0.0 | $3.20 \pm 0.09$ | $-2.35 \pm 0.11$ | PW |
| 0.4950 | 0.10 | $2.21 \pm 0.04$ | $-1.27 \pm 0.03$ | PW |
| 0.4785 | 0.20 | $1.50 \pm 0.04$ | $-0.53 \pm 0.005$ | PW |
| 0.476 | 0.30 | $1.18 \pm 0.02$ | $-0.21 \pm 0.005$ | PW |
| 0.484 | 0.40 | — | $-0.105 \pm 0.005$ | PW |
| 0.500 | 0.50 | $0.93 \pm 0.01$ | $-0.039 \pm 0.002$ | PW |
| 0.500 | 0.50 | 0.95 | $-0.039$ | [2, 5] |

(a)

N(t)

p=0.10

t

(b)

P(t)

p$_C$=0.10
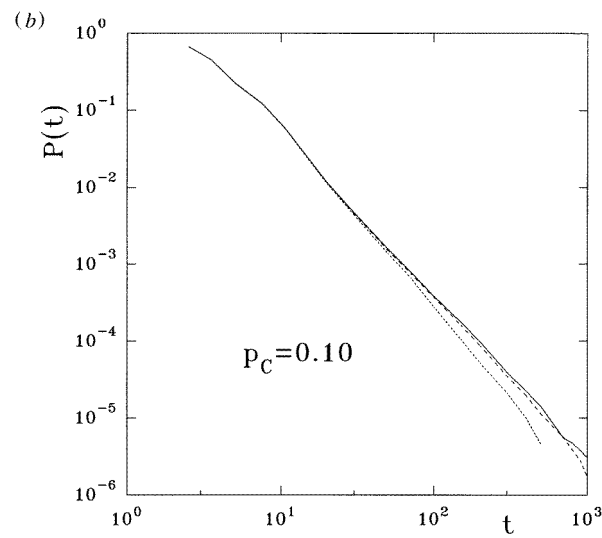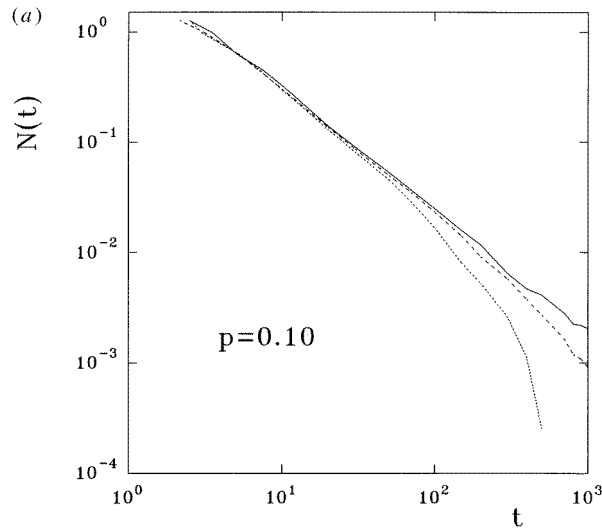
**Figure 5.** Log–log plots of (a) $N(t)$ and (b) $P(t)$ versus $t$ obtained taking $Y_C = 0.10$ and scanning $Y_A$. $Y_A = 0.4945$ (upper curves, supercritical), $Y_A = 0.4950$ (middle curves, criticality) and $Y_A = 0.4955$ (lower curves, subcritical).

hand, for $Y_A = Y_C = \frac{1}{2}$, the DMM model is mapped onto the MM model and the results of the present work are also in excellent agreement with previously reported values (see the last two rows of table 1).

It is interesting to note that critical exponent values can be tuned by varying the parameters $[Y_A, Y_C]$ and the crossover from the DMM model to the MM model is smooth (see figure 6 and table 1). Similarly, Evans *et al* [15] have found that the same exponents for the DM model can also be tuned when the rate of reaction varies. Also, simulations of the DM model assuming that the dimer adsorbs according to the 'hot dimer' deposition mechanism indicate that the exponents $\eta$ and $\delta$ at first-order IPTs can be tuned by varying the distance which each of the monomers can take resulting from hot dimer dissociation [29].

It has been established that second-order IPTs into absorbing or poisoned states generically belong to the universality class of directed percolation [13, 28]. Our epidemic analysis at the continuous IPTs of the DMM model gives critical exponents in full agreement

(a)

N(t)

$10^0$

$10^{-1}$

$10^{-2}$

$10^0$   $10^1$   $10^2$   t

(b)   $10^0$

P(t)

$10^{-1}$

$10^{-2}$

$10^{-3}$

$10^{-4}$

$10^{-5}$

$10^{-6}$

$10^0$   $10^1$   $10^2$   $10^3$

t

**Figure 6.** Log–log plots of (a) $N(t)$ and (b) $P(t)$ versus $t$ obtained at criticality. The lower and upper curves correspond to the DM and MM models, respectively. Intermediate curves correspond to the critical points listed in table 1. The obtained critical exponents from the asymptotic behaviour of the plots are also listed in table 1.

with these findings. As in the case of standard second-order reversible transitions, this behaviour can be understand considering that the correlation length ($\xi$) diverges when approaching criticality and consequently $\xi$ is the only relevant length scale. Microscopic details of the models, with length scales much shorter than $\xi$, become overlapped and consequently they are irrelevant. This mechanism is the origin of universality. In contrast, correlations are short range close to first-order IPTs and consequently microscopic details of the models are relevant: universality is not observed and each pair of critical points has its own set of critical exponents as, for example, is shown in table 1.

Due to the lack of a satisfactory theory capable of describing first-order IPTs in reaction systems, the explanation of the obtained results on the basis of analytical arguments is not yet possible. However, the physical picture behind the epidemic analysis performed can be understood in terms of the description outlined by Evans *et al* [15, 16]. Our epidemic analysis reveals that, within the reactive regime and even very close to the critical point, most of the initially empty blobs embedded in the poisoned state quickly become poisoned

(see, for example, figures 5 and 6). However, later on a few surviving epidemic blobs eventually prevail, spreading the reactive steady state across the entire sample. The large positive $\delta$ values and the large negative $\eta$ values (see table 1) reveal a greatly reduced epidemic survivability. In contrast, the conventional epidemic behaviour characteristic of directed percolation-type continuous transitions produces small positive values for $\delta$ and $\eta$.

## 5. Conclusions

The critical behaviour of a dimer–monomer–monomer (DMM) model involving one dimer and two different monomers is studied. The DMM model has a continuous set of both second- and first-order irreversible phase transitions (IPTs). Critical points are precisely determined by means of an epidemic analysis which also allows us to evaluate dynamic critical exponents. These exponents confirm that second-order IPTs belong to the universality class of directed percolation, while universality is not found at first-order IPTs. The dynamic exponents of the first-order IPTs cross over, along the critical line, between the values characteristic of the DM model and those of the MM model.

Further investigations of generalized versions of the DMM model, e.g. to account for surface diffusion, desorption, hot-dimer deposition, different rate constants, lateral interactions, etc, will be addressed in future works.

## Acknowledgments

## References

 [1]  Liggett T M 1985 *Interacting Particle Systems* (Berlin: Springer)
 [2]  Evans J W 1992 *Langmuir* **7** 2514
 [3]  Zhdanov V P and Kasemo B 1994 *Surf. Sci. Rep.* **20** 111
 [4]  Ziff R M, Gulari E and Barshad Y 1986 *Phys. Rev. Lett.* **56** 2553
 [5]  Meakin P and Scalapino D J 1987 *J. Chem. Phys.* **87** 731
 [6]  Chopard B and Droz M 1988 *J. Phys. A: Math. Gen.* **21** 205
 [7]  ben-Avraham D, Considine D, Meakin P, Redner S and Takayasu H 1990 *J. Phys. A: Math. Gen.* **23** 4297
 [8]  Jensen I and Fogedby H C 1990 *Phys. Rev.* A **42** 1969
 [9]  Albano E V 1990 *J. Phys. A: Math. Gen.* **23** L545
[10]  Albano E V 1990 *Phys. Rev.* B **42** R10818
[11]  Albano E V 1990 *Surf. Sci.* **235** 351
[12]  Mai J and von Niessen W 1990 *J. Chem. Phys.* **93** 3685
[13]  Mai J and von Niessen W 1991 *Phys. Rev.* A **44** R6165
[14]  Jensen I, Fogedby H C and Dickman R 1990 *Phys. Rev.* A **41** R3411
[15]  Albano E V 1991 *J. Chem. Phys.* **94** 1499
[16]  Evans J W and Miesch M S 1991 *Phys. Rev. Lett.* **66** 833
[17]  Evans J W and Miesch M S 1991 *Surf. Sci.* **245** 401
[18]  Ziff R M and Brosilow B J 1992 *Phys. Rev.* A **46** 4630
[19]  Evans J W and Ray T R 1994 *Phys. Rev.* E **50** 4302
[20]  Mai J, Casties A and von Niessen W 1992 *Chem. Phys. Lett.* **196** 358
[21]  Albano E V 1994 *Phys. Rev. Lett.* **72** 108
[22]  Kim M H and Park H 1994 *Phys. Rev. Lett.* **73** 2579
[23]  Albano E V 1994 *Phys. Rev.* E **50** 1129

[24] Kang H C and Weinberg W H 1993 *Phys. Rev.* E **47** 1604; **48** 3464
[25] Warnatz J 1981 *Chemistry of Statinary and Non-stationary Combustions* (Springer Series in Chemical Physics **18**) ed K H Ebert, P Deuflhard and W Jager (Berlin: Springer) p 162
[26] Albano E V 1994 *Surf. Sci.* **306** 240
[27] Albano E V 1994 *J. Phys. A: Math. Gen.* **27** 3751
[28] Albano E V 1995 *Physica* **214A** 426
[29] Grassberger P and de la Torre A 1979 *Ann. Phys., NY* **122** 373
[30] Albano E V and Pereyra V D 1994 *J. Phys. A: Math. Gen.* **27** 7763